THE JOURNAL OF BIOLOGICAL CHEMISTRY
Vol. 275, No. 25, Issue of June 23, pp. 19068–19075, 2000

Printed in U.S.A.

Acyclic Permutants of Naturally Occurring Cyclic Proteins

CHARACTERIZATION OF CYSTINE KNOT AND β-SHEET FORMATION IN THE MACROCYCLIC POLYPEPTIDE KALATA B1*

Received for publication, January 20, 2000, and in revised form, March 21, 2000
Published, JBC Papers in Press, March 27, 2000, DOI 10.1074/jbc.M000450200

Norelle L. Daly and David J. Craik‡

From the Centre for Drug Design and Development, Institute for Molecular Bioscience, University of Queensland, Brisbane QLD 4072, Australia

Kalata B1 is a prototypic member of the unique cyclotide family of macrocyclic polypeptides in which the major structural features are a circular peptide backbone, a triple-stranded β-sheet, and a cystine knot arrangement of three disulfide bonds. The cyclotides are the only naturally occurring family of circular proteins and have prompted us to explore the concept of acyclic permutation, *i.e.* opening the backbone of a cross-linked circular protein in topologically permuted ways. We have synthesized the complete suite of acyclic permutants of kalata B1 and examined the effect of acyclic permutation on structure and activity. Only two of six topologically distinct backbone loops are critical for folding into the native conformation, and these involve disruption of the embedded ring in the cystine knot. Surprisingly, it is possible to disrupt regions of the β-sheet and still allow folding into native-like structure, provided the cystine knot is intact. Kalata B1 has mild hemolytic activity, but despite the overall structure of the native peptide being retained in all but two cases, none of the acyclic permutants displayed hemolytic activity. This loss of activity is not localized to one particular region and suggests that cyclization is critical for hemolytic activity.

Circular permutation is a conceptually intriguing tool that has been applied in recent years for the study of protein folding. It involves the synthesis or expression of proteins in which the position of the N and C termini are permuted from their native locality. It may be thought of as joining the ends of a protein and then opening the chain elsewhere. These experiments have shown that it is possible in some cases to permute the termini of a protein and still allow folding into the native conformation (1, 2), thus providing valuable information on protein folding. In practice the conceptual "circular proteins" intrinsic to the design of circular permutants are never actually synthesized but are theoretical intermediates. The recent discovery of a naturally occurring family of circular proteins, however, allows us to start from a circular protein and explore the concept of "acyclic permutation." In the current study we introduce this concept for the prototypic circular protein, kalata B1, the first circular protein to be structurally characterized.

* This work was supported in part by a grant from the Australian Research Council (ARC) (to D. J. C.). The Institute for Molecular Bioscience is a special research center of the ARC. The costs of publication of this article were defrayed in part by the payment of page charges. This article must therefore be hereby marked "*advertisement*" in accordance with 18 U.S.C. Section 1734 solely to indicate this fact.

‡ An Australian Research Council Senior Fellow. To whom correspondence should be addressed. Tel.: 61-7-3365-4945; Fax: 61-7-3365-2487; E-mail: d.craik@mailbox.uq.edu.au.

Kalata B1 belongs to a family of macrocyclic peptides termed the cyclotides (3) that are approximately 30 amino acids in length with three disulfide bonds and are isolated from plants in the Rubiaceae and Violaceae families (4–7). These peptides display an interesting range of biological activities, which led to their initial discovery. The circulins were found in a screen for anti-human immunodeficiency virus activity (8), cyclopsychotride A inhibits neurotensin binding to cell membranes (9), and kalata B1 shows uterotonic activity (6, 10). Violapeptide I (11) was originally discovered based on its hemolytic activity, and it has recently been shown that kalata B1 (12, 13), the circulins (12, 13), and cyclopsychotride A (13) also have relatively weak hemolytic activity. A large number of additional peptides from this family have recently been discovered. The varv peptides A-H have been isolated from *Viola arvensis* (14, 15), and we have reported the discovery of several peptides from *Viola odorata*, *Viola hederaceae*, and *Oldenlandia affinis* (3). There is approximately 40% sequence conservation throughout the known sequences. The importance of this family of unusually large cyclic peptides has been increased by the discovery of their anti-microbial activity against various strains of bacteria and fungi (13).

The three-dimensional structures of three members of this family (kalata B1 (10), circulin A (16), and cycloviolacin O1 (3)) have been determined by NMR spectroscopy and reveal the presence of a cyclic cystine knot motif, so named because of the N- to C-cyclized backbone and knotted three-dimensional structure (3, 12). The disulfide bonds are in a cystine-knot arrangement with the Cys connectivities I-IV, II-V, and III-VI (10, 17) in which two disulfide bonds and their connecting backbone segments produce an eight-residue cycle through which the third disulfide bond "threads" (10). The threading of this embedded eight-residue cycle is highlighted in Fig. 1. The cyclic cystine knot motif is distinct because of its cyclic backbone; however, the cystine knot motif is present in a large number of peptides and proteins with diverse functions. These include ion channel toxins (18), proteinase inhibitors (18), and growth factors (19), and it has recently been suggested that a phenoloxidase inhibitor is also a member of this family (20). It is therefore of great interest to explore the folding of this important motif.

Numerous other peptide families contain characteristic cystine frameworks (*i.e.* the positions and spacings between the cysteine residues) that appear to stabilize structural motifs (21), and thus, it is interesting to examine the effect of changing the cystine framework on folding and structure. Permuting the termini of acyclic derivatives of kalata B1 effectively alters the cystine framework, and thus, this study has broader implications than just for cystine knot peptides.

We have previously reported the synthesis and folding of

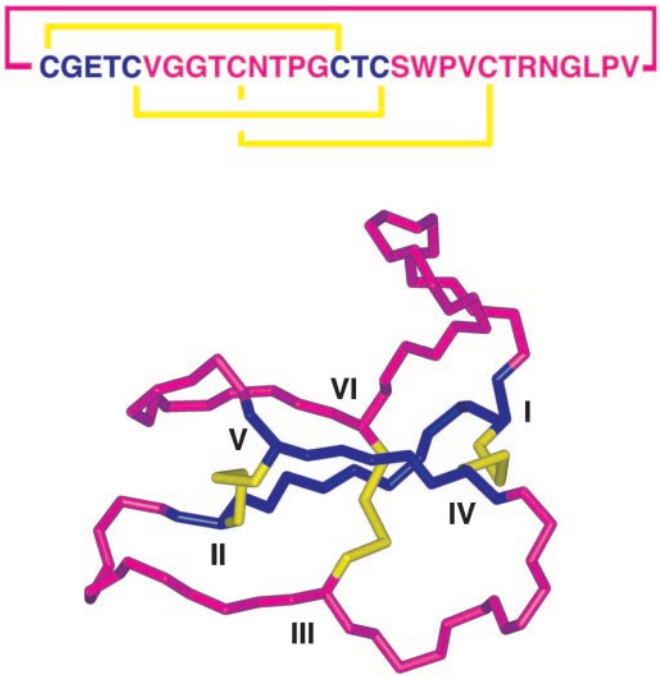

FIG. 1. **The sequence and three-dimensional structure of kalata B1.** The eight-residue loop formed by the disulfide bonds I-IV and II-V is highlighted in *blue* with the rest of the backbone shown in *pink*, and the cysteine side chains shown in *yellow*.

kalata B1 using two separate strategies (12), one in which the disulfide bonds were formed before cyclization, and the other in which cyclization preceded oxidation of the cysteine residues. These two strategies allowed a comparison of the folding of kalata B1 in the linear and cyclic forms. Cyclization appeared to have a dramatic effect on folding, as oxidation of cyclic-reduced kalata B1 produced the correctly folded peptide in aqueous solution, in contrast to the case for the linear form where oxidation in water produced mainly misfolded products. However, a significant proportion of correctly folded peptide was obtained from the linear precursor when oxidation reactions were performed in the presence of organic solvents. A hydrophobic solution environment appeared to be required to stabilize the surface-exposed hydrophobic residues that are formed upon folding into the native conformation (12). Furthermore, hemolytic activity was observed for cyclized kalata B1 but not for the oxidized linear derivative (12). These results implied that cyclization was either very important for activity or that the particular backbone segment that was opened in the linear derivative was important for maintaining activity. It was evident that further linear analogues were required to resolve this question. In the current study we have synthesized the complete suite of topologically distinct acyclic permutants of kalata B1. The effects of acyclic permutation on folding, structure, and activity are examined.

EXPERIMENTAL PROCEDURES

Synthesis of Acyclic Permutants of Kalata B1—Permutants of kalata B1 were assembled using manual solid phase peptide synthesis with *tert*-butoxycarbonyl chemistry on a 0.5-mmol scale. *p*-Methylbenzhydrylamine or 4-(oxymethyl)phenylacetamidomethyl resin was used (Applied Biosystems, Foster City, CA), and amino acids were added to the resin using 2-(1H-benzotriazol-1-yl)-1,1,3,3-tetramethyluronium with *in situ* neutralization (22). Cleavage of the peptide from the resin was achieved using hydrogen fluoride (HF) with cresol and thiocresol as scavengers (HF:cresol:thiocresol; 9:1:1 v/v). The reaction was allowed to proceed at −5–0 °C for 1 h. After cleavage, the peptides were dissolved in 50% acetonitrile, 0.1% trifluoroacetic acid and lyophilized. The crude, reduced peptides were purified using preparative reverse-phase HPLC (RP-HPLC)[1] on a Vydac C18 column. Gradients of 0.1% aqueous trifluoroacetic acid and 90% acetonitrile, 0.09% trifluoroacetic acid were employed with a flow rate of 8 ml/min, and the eluant was monitored at 230 nm. These conditions were used in the subsequent purification steps. Mass analysis was performed on a Sciex (Thornhill, Ontario) triple quadrupole mass spectrometer using electrospray sample ionization.

Disulfide Formation—Oxidation reactions were performed using the best conditions established for the cyclic peptide (12). The purified reduced peptides were dissolved in 50% 2-propanol, 1–10 mM reduced glutathione in 0.1 M ammonium bicarbonate (pH 8.5). The reactions were left at room temperature for 24 h. The pH was lowered with trifluoroacetic acid before purification with RP-HPLC.

NMR Spectroscopy—Samples for ^{1}H NMR measurements contained 1 mM peptide in either 99.99% ^2H_2O or 90% H_2O, 10% ^2H_2O (v/v) at ~pH 4. ^2H_2O (99.9% and 99.99%) was obtained from Cambridge Isotope Laboratories, Woburn, MA. Spectra were recorded at 12 °C and 25 °C on a Bruker ARX-500 spectrometer equipped with a shielded gradient unit. Low temperature studies employed a temperature-controlled stream of cooled air using a Bruker BCU refrigeration unit and a B-VT 2000 control unit. Two-dimensional NMR spectra were recorded in phase-sensitive mode using time-proportional phase incrementation for quadrature detection in the t_1 dimension (23). The two-dimensional experiments included DQF-COSY (24), TOCSY (25) using a MLEV-17 spin lock sequence (26) with a mixing time of 80 ms, and NOESY (27) with mixing times of 200 ms and 250 ms. For DQF-COSY experiments, solvent suppression was achieved using selective low power irradiation of the water resonance during a relaxation delay of 1.8 s. Solvent suppression for NOESY and TOCSY experiments was achieved using a modified WATERGATE (water suppression by gradient-tailored excitation) sequence (28). Spectra were routinely acquired over 6024 Hz with 4096 complex data points in F_2 and 512 increments in the F_1 dimension. Slowly exchanging NH protons were detected by acquiring a series of one-dimensional and TOCSY spectra of the fully protonated peptide immediately after dissolution in ^2H_2O. Exchange rates for amide protons were determined using these spectra, with the volumes measured using XWINNMR and normalized to a non-exchangeable proton. The exchange rates were calculated by fitting the volume of the decaying signals over time to the equation $I = I_o \exp(-k_{ex} \times t) + I(\infty)$ (29). $^3J_{\alpha HNH}$ coupling constants were measured either from one-dimensional spectra or from DQF-COSY spectra transformed to 8192 × 1024 over the region of interest.

Spectra were processed on a Silicon Graphics Indigo workstation using XWINNMR (Bruker) software. The t_1 dimension was zero-filled to 2048 real data points, and 90° phase-shifted sine bell window functions were applied before Fourier transformation. Chemical shifts were referenced to DSS at 0.00 ppm.

Hemolytic Activity Assay—Human erythrocytes (blood group O) were washed several times with phosphate-buffered saline and centrifuged at 3500 rpm until a clear supernatant was obtained. A 1% solution of the red blood cells in phosphate-buffered saline was used in the assays, which were performed by adding 20 μl of test compound to 80 μl of the 1% suspension of red blood cells. A 1% solution of SDS was used as a control for 100% hemolysis (30). The mixtures were left at room temperature for 1 h and then centrifuged at 3500 rpm for 1 min. The supernatant (20 μl) was diluted with 580 μl of deionized (Milli-Q) water, and the absorbance was measured at 415 nm.

RESULTS

There are six cysteine residues in peptides from the cyclotide family and, hence, six loops in the backbone that can be opened to form six topologically distinct acyclic permutants. We have synthesized a series of truncated acyclic permutants of kalata B1 in which each of the six loops has been opened to examine the effects of acyclic permutation on folding, structure, and activity. A schematic representation of the acyclic permutants is shown in Fig. 2. In general the permutants were designed to include one residue adjacent to each of the two cysteine residues spanning the cut site, with any intervening residues de-

[1] The abbreviations used are: RP-HPLC, reversed-phase high performance liquid chromatography; TOCSY, two-dimensional total correlation spectroscopy; NOE, nuclear Overhauser effect; NOESY, two-dimensional NOE spectroscopy; DQF-COSY, double quantum filtered correlation spectroscopy; DSS, sodium 2,2-dimethyl-2-silapentane-5-sulfonate.

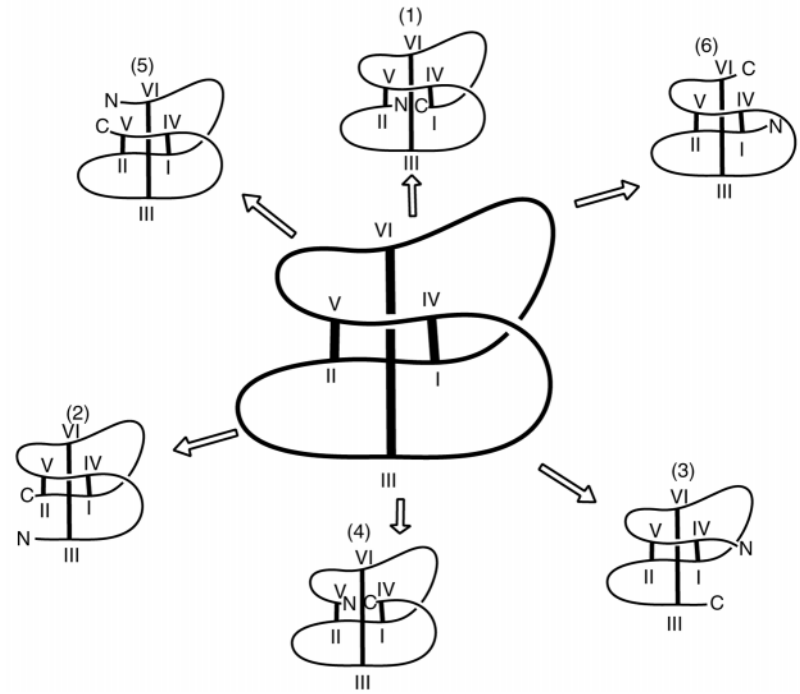

FIG. 2. **A schematic representation of the three-dimensional structure of kalata B1 (*middle* of *diagram*) and the six acyclic permutants produced upon opening of the six loops between the cysteine residues.** The *numbers* in *parentheses* represent the loops that are opened.

leted. However, in some cases only a single residue was deleted or the permutants contain the entire amino acid sequence of kalata B1 but are acyclic. The sequences and nomenclature of the seven permutants synthesized are shown in Table I. Since the parent protein is cyclic, the choice of the numbering system for amino acid residues is arbitrary, but we have followed that introduced earlier by Daly *et al.* (16). However, since our focus here is on the concept of acyclic permutation, it is also convenient to refer to individual peptides via the backbone loop that is removed, (**1–6**), as summarized in Table I and Fig. 2. Single permutants were made for loops 1–5, and two acyclic permutants were made for loop 6: **6a**, which corresponds to complete removal of the loop, and **6b**, in which the loop is cut but no residues are removed.

All permutants, with the exception of kalata B1(8–7), *i.e.* **2**, were synthesized on *p*-methylbenzhydrylamine resin to produce a C-terminal amide upon cleavage with HF. This peptide was available from a previous study (12) on the total chemical synthesis of kalata B1, where the linear peptide was synthesized with a free C terminus to allow cyclization. The N termini of the permutants were unprotected and, hence, positively charged.

The permutants of kalata B1 were assembled using manual solid phase peptide synthesis and subsequently purified using RP-HPLC before oxidation. The oxidation conditions were chosen based on our previous studies (12) on the synthesis of kalata B1, which revealed that cyclic, reduced kalata B1 folds very efficiently in 0.1 M ammonium bicarbonate (pH 8), 1 mM reduced glutathione in 50% (v/v) 2-propanol at room temperature. Applying these oxidation conditions to the folding of the kalata B1 permutants enabled a comparison of the efficiency of folding and allowed the effect of opening the loops of the parent circular molecule to be assessed.

The HPLC traces used to monitor the folding reactions of the acyclic permutants of kalata B1 are given in Fig. 3. We have shown previously (12) that correctly folded kalata B1 elutes significantly later than the reduced circular peptide because of a large patch of surface-exposed hydrophobic residues in the native conformation (10). The RP-HPLC trace for folding of the circular form is, thus, included in Fig. 3 for comparison. Inspection of the traces for the new acyclic permutants shows that in all but two cases a sharp, late-eluting peak is observed together with a set of broader, earlier-eluting peaks. It appears likely that the sharp peaks (marked *N** in Fig. 3) correspond to native-like folds and that the broader peaks correspond to misfolded derivatives. This interpretation is consistent with our earlier study (12) of kalata B1(8–7), which we used as a precursor in the synthesis of circular kalata B1. There we noted that linear kalata B1(8–7) displays similar HPLC properties to the cyclic peptide, in that the reduced form elutes much earlier than the correctly folded form, which yields a sharp, late-eluting peak. The misfolded forms had broad peaks that were poorly resolved and were much more hydrophilic than the correctly folded form, as shown by their shorter retention times.

The absence of late-eluting peaks for des-3-kalata B1 (**1**) and

TABLE I
Acyclic permutants of kalata B1

The native sequence is backbone-cyclized. The N and C termini of the acyclic permutants are in bold. The nomenclature chosen describes the residues deleted, or in the case of the full length, non-cyclic permutants, the residue numbers of the N and C termini are in parentheses. The numbers in parentheses after the name of the permutant refer to the loop that is perturbed, with des-(23–28)-kalata B1 and kalata B1(24–23) designated **6a** and **6b**, respectively.

1 5 10 15 20 25		
CGETCVGGTCNTPGCTCSWPVCTRNGLPV	Native Kalata B1	
–C**G** **T**CVGGTCNTPGCTCSWPVCTRNGLPV–	Des-(3)-kalata B1	**(1)**
–CGETCV**GG**TCNTPGCTCSWPVCTRNGLPV–	Kalata B1-(8-7)	**(2)**
–CGETCVGGTC**N** **G**CTCSWPVCTRNGLPV–	Des(12-13)-kalataB1	**(3)**
–CGETCVGGTCNTPG**C** **C**SWPVCTRNGLPV–	Des(16)-kalata B1	**(4)**
–CGETCVGGTCNTPGCTC**S** **V**CTRNGLPV–	Des(19-20)-kalata B1	**(5)**
–CGETCVGGTCNTPGCTCSWPVC**T** **V**–	Des(24-28)-kalata B1	**(6a)**
–CGETCVGGTCNTPGCTCSWPVC**TR**NGLPV–	Kalata B1-(24-23)	**(6b)**
Loop 1 Loop 2 Loop 3 Loop 4 Loop 5 Loop 6		

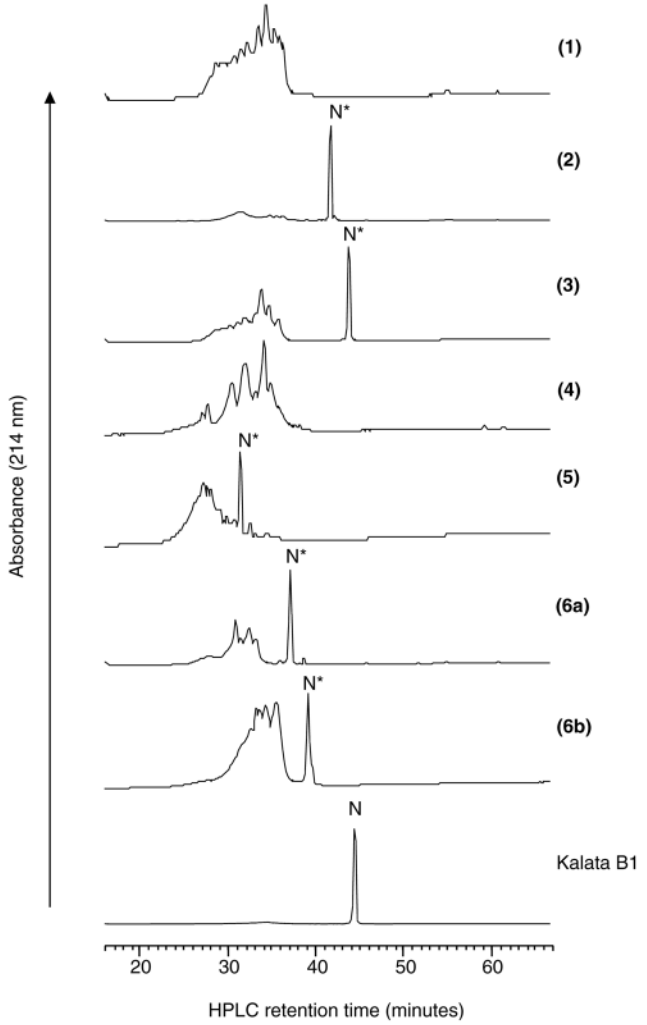

FIG. 3. **HPLC traces of oxidation reactions on the synthetic acyclic permutants of kalata B1.** Linear reduced peptides were oxidized in 50% 2-propanol, 1 mM reduced glutathione in 0.1 M ammonium bicarbonate (pH 8). The reactions were conducted at room temperature for 24 h. The correctly folded forms are labeled with *N**. Oxidation of cyclic, reduced peptide (*N*) is included in the diagram for comparison.

des-(16)-kalata B1 (**4**) suggests that correctly folded peptides are not formed in these cases. In an attempt to find conditions where des-(3)-kalata B1 and des-(16)-kalata B1 produce a similar folding pattern to the other permutants and to the native peptide, several conditions were varied, including the buffer, temperature, length of oxidation, and presence of denaturants. However, the HPLC traces from these reactions did not differ significantly from those shown in Fig. 3. These results imply the regions between Cys-1 and Cys-5, and Cys-15 and Cys-17, which correspond to loops 1 and 4 (Table I), are structurally very important. Opening the peptide chain in these loop segments produces a fundamental change in the ability of the molecule to fold to a native-like conformation. By contrast, the other four loops can be cut and still allow folding into the native conformation.

NMR Spectroscopy—To further characterize the conformations of the folded forms associated with the late- eluting peaks, they were purified by RP-HPLC and studied by ^{1}H NMR spectroscopy. TOCSY and NOESY spectra were recorded for the acyclic permutants **2**, **3**, **5**, **6a**, and **6b**, and resonance assignments were obtained using established techniques (31).

Chemical shifts are extremely sensitive to structural changes and, thus, an analysis of the chemical shifts was first used to compare the structures of the permutants. Fig. 4 shows the differences in αH chemical shifts between the acyclic permutants and the native peptide. For most residues, the permutants have similar shifts to the native peptide, indicating that the overall three-dimensional structure is retained. This confirms the finding from the HPLC data that it is possible to produce correctly folded acyclic permutants.

In general, the largest chemical shift differences are near the introduced termini, as might be expected because of the breakage of a peptide bond and the introduction of new charges; however, other differences also exist. The most significant are in kalata B1(24–23), *i.e.* **6b**, the permuted derivative where loop 6 is opened. In this case the large chemical shift changes over residues 23–29 relative to the native peptide reflect an untethering of loop 6. The chemical shifts in this region of the acyclic permutant are much closer to random coil values than they are in the native peptide, consistent with local structuring of this region in the native circular protein but disorder in the open chain derivative. This conclusion is also consistent with the HPLC retention time for this permutant, which is significantly faster than for the native peptide despite having the same amino acid composition and with chemical shift data for the truncated permutant, **6a**. Most of the residues in loop 6 are removed in the truncated permutant, and the expected large changes in chemical shifts occur at the new terminal residues, 23 and 29, but other residues are unaffected.

Putting aside these local conformational changes due to the introduction of breaks in the circular protein backbone, the very significant finding to emerge from the αH chemical shift analysis is that the overall structures of the folded acyclic permutants are very similar to that of the native circular protein. Circularization is not essential for correct folding.

Changes in βH chemical shifts were also found to be extremely useful for comparing structures of the permutants, particularly for Cys side-chain conformations. The chemical shift separation of the two β-protons in each AMX spin system in the permutants was measured, and the values were subtracted from the corresponding shift separations in the native peptide. The results are shown in Fig. 5, but before examining these relative changes in βH shift separations, it is useful to examine the base-line values in the native peptide. In kalata B1 the βH chemical shift separations for individual AMX residues range from 0.0 ppm (Asn-11, Ser-13, Trp-19) to 1.20 ppm (Cys-15) and are typically 0.35 $\pm$ 0.1 ppm for the other Cys residues. In general, the larger the βH chemical shift separation for an individual methylene pair of protons, the more likely that pair is located in a highly structured environment. A decrease in shift separation in a permutant relative to the native peptide indicates a change to a more disordered environment.

Fig. 5 shows that most of the changes in shift separations are indeed negative in sign, so that permutation does in general lead to decreased order in side-chain environments. The effects are very small for kalata B1(8–7) (**2**) and des-(19–20)-kalata B1 (**5**), whose βH shift separations are within 0.2 ppm of the native peptide, confirming that there are no significant structural changes associated with opening of loops 2 or 5. There are more significant differences for des-(12–13)-kalata B1 (**3**), des-(24–28)-kalata B1 (**6a**), and kalata B1(24–23) (**6b**), particularly at Cys-15. Opening of loop 3 or 6 thus appears to have a greater effect on disulfide bond geometry than does opening loop 2 or 5. Interestingly, increased βH shift separations are observed in most of the permutants for Cys-10 and Cys-22, which make up the "penetrating" disulfide bond.

A range of additional structural data was also measured for the various permutants, including the location of hydrogen bonds, inferred from slow exchange amide data, long range $\alpha\alpha$

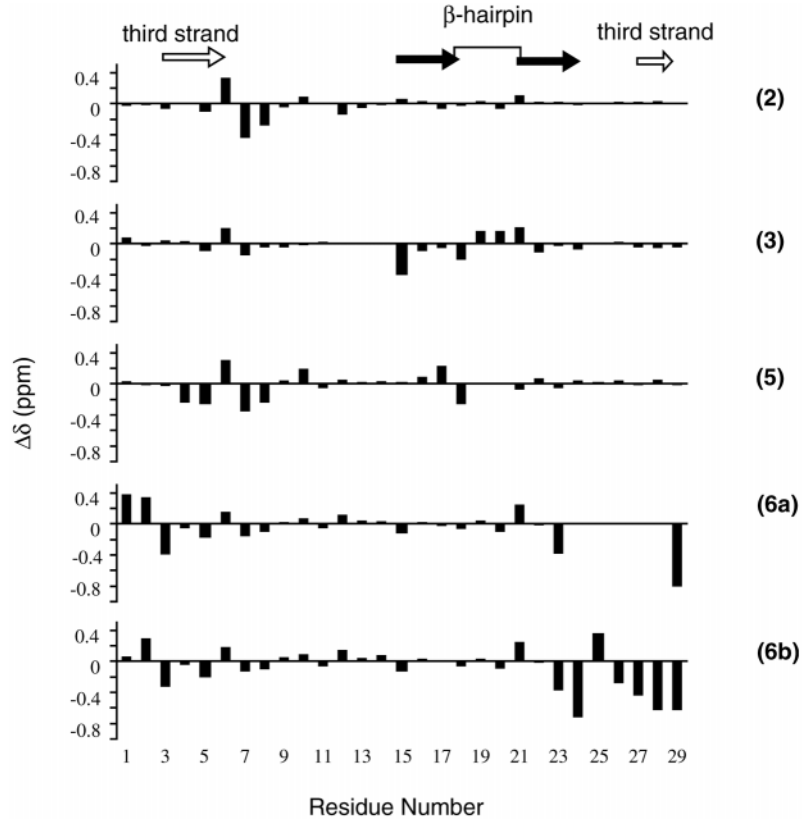

FIG. 4. **αH chemical shift differences between the acyclic permutants of kalata B1 and native kalata B1.** Only the four permutants that produced late-eluting peaks were analyzed. The chemical shifts were measured from TOCSY spectra recorded on a Bruker ARX 500 MHz spectrometer at 298 K and are referenced to internal DSS. *Arrows* above the shifts represent the secondary structure; the *black arrows* represent the β-hairpin, and the *white arrows* represent the distorted strand, which has a β-bulge present.

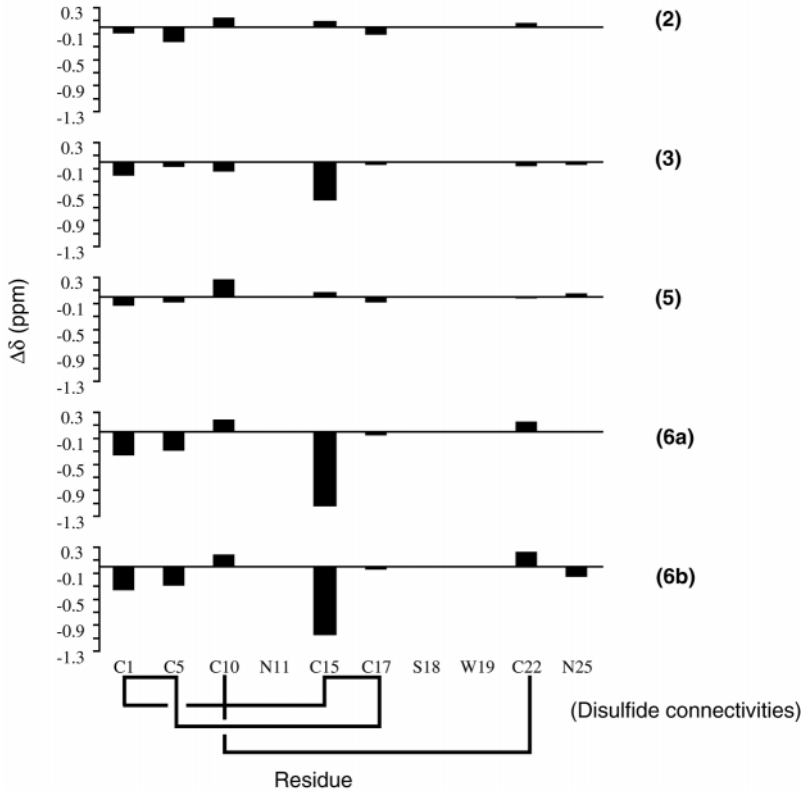

FIG. 5. **Differences in the separation of the two β protons in the AMX spin systems in the acyclic permutants of kalata relative to the shift separation in native kalata B1.** The chemical shifts were measured from TOCSY spectra recorded on a Bruker ARX 500 MHz spectrometer at 298 K and are referenced to internal DSS. The disulfide connectivities, based on the native peptide, are shown at the bottom of the figure to facilitate tracking of trends for connected cysteine residues.

NOEs indicative of β-sheet, and $^3J_{\alpha HNH}$ coupling constants indicative of β-strands. A summary of the secondary structure elements present in the permutants as deduced from these data is given in Fig. 6. These are broadly consistent with the chemical shift analysis and indicate that a significant degree of native secondary structure is maintained in most of the acyclic permutants. Des-(12–13)-kalata B1 (**3**) appears to be the least structured of the folded forms, but even it contains many large (>8.5 Hz) $^3J_{\alpha HNH}$ coupling constants and a cross-sheet αα NOE, consistent with significant maintenance of the sheet. The sheet in this permutant appears to be subject to more breathing motions than in the native peptide, however, as no slowly exchanging amide protons were detected. In the other folded permutants most of the native hydrogen bonds were maintained.

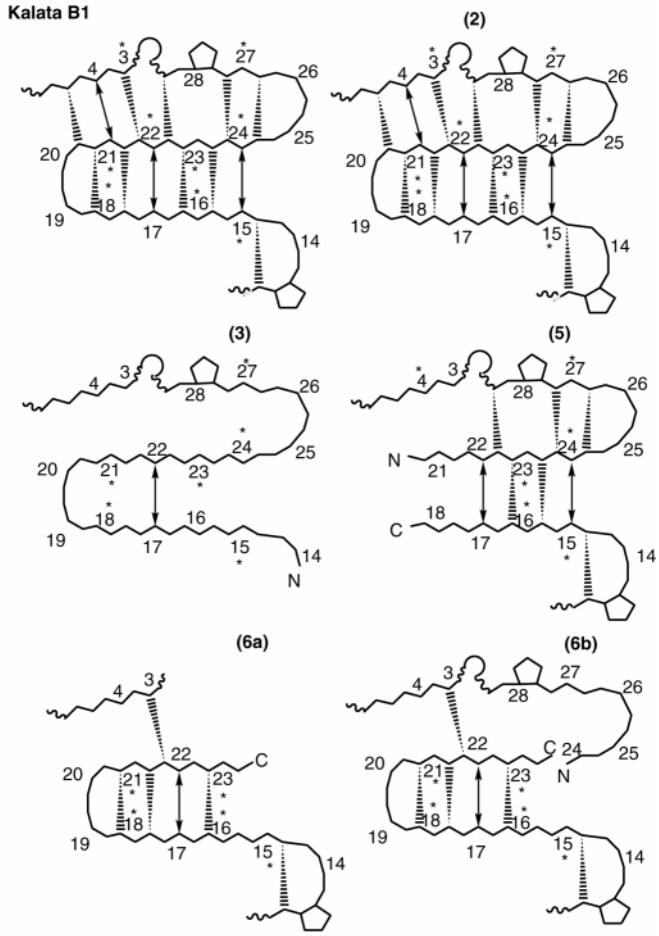

FIG. 6. **Summary of experimental NMR data used to determine the β-sheet regions of the acyclic permutants of kalata B1.** The hydrogen bonds, deduced from slow exchange data, are represented as *dashed lines*, with the narrow end corresponding to the hydrogen bond donor and the wider end corresponding to the hydrogen bond acceptor. Observed αH-αH NOEs across the sheet are shown as double-headed *arrows*, and residues with large (>8.5 Hz) $^3J_{\alpha HNH}$ coupling constants are highlighted with *asterisks*.

The amide exchange rates for native kalata B1 and the acyclic permutants are given in Table II. Des-(12–13)-kalata B1 (**3**) is not included as the amide signals were exchanged within 25 min of dissolving in ^2H_2O. Des-(19–20)-kalata B1 (**5**), des-(24–28)-kalata B1 (**6a**), and kalata B1(24–23) (**6b**) in general have exchange rates higher than that observed for the native peptide, suggesting that the overall stability has been decreased. In contrast, kalata B1(8–7) (**2**) has exchange rates closer to those observed for the native peptide, which implies that opening the peptide backbone in loop 2 does not significantly affect the stability.

In summary, the combined NMR and HPLC data showed that only two of the six topologically distinct acyclic permutants did not fold, and these were associated with cuts to loops 1 or 4. Acyclic permutants with cuts to the other four loops folded similarly to the native circular protein.

Hemolytic Activity—The cyclotides have a diverse range of biological activities, but their natural function within plants is not yet known. Membrane disruption is potentially a common feature of these various activities, and so it was convenient to use a hemolytic assay to monitor the biological effects of acyclic permutation. Kalata B1 has previously been shown to have hemolytic activity (12, 13), and this was confirmed in the current study, where 50% hemolysis occurs on incubation of erythrocytes with 50 μM kalata B1. Recent studies have shown that

TABLE II

Experimental amide exchange rates (k_{ex}, min^{-1}) for native kalata B1 and the acyclic permutants

Des-(12–13)-kalata B1 was not included because all amide signals had exchanged within 25 min of dissolving in ^2H_2O. A dash indicates the residue was not present.

Residue	k_{ex}				
	Native kalata B1	Kalata B1-(8–7)	Des-(19–20)-kalata B1	Des-(24–28)-kalata B1	Kalata B1(24–23)
			10^{-3} min^{-1}		
Cys-5	2.7	8.9	>40	>40	>40
Cys-15	1.1	1.7	1.6	31	8.6
Thr-16	2.3	1.7	27	>40	>40
Ser-18	0.37	7.7	>40	38	18
Val-21	1.6	1.3	[a]	6.0	5.3
Cys-22	0.83	1.7	>40	10	9.0
Thr-23	0.63	1.5	7.1	13	8.2
Arg-24	3.3	4.8	17	—	[a]
Leu-27	2.9	3.9	6.6	—	>40
Val-29	1.3	1.7	8.3	[a]	>40

[a] An N-terminal residue.

factors such as high amphipathicity, high hydrophobicity, and high helicity correlate with high hemolytic activity (32). Thus, it is not surprising that the level of hemolytic activity observed for the non-helical kalata B1 is rather mild and less than that for highly helical peptides such as melittin (<1 μM for 50% hemolysis) (33). However, despite the ready detection of activity for the parent kalata molecule, no lysis was observed for the acyclic permutants at concentrations of up to ~60 μM. Thus it appears that circularization of the backbone is not required for correct folding but is required for hemolytic activity.

DISCUSSION

This examination of the *in vitro* folding of acyclic permutants of the cyclotide peptide, kalata B1, has highlighted some important features required for folding. We have essentially opened kalata B1 within each of the six loops spanning consecutive cysteine residues and have found a characteristic pattern of folded forms upon oxidation of the cysteine residues as determined by RP-HPLC and NMR spectroscopy. In general, the folded forms elute significantly closer to the native material and much later than misfolded forms. The misfolded forms also yield broad HPLC peaks compared with the correctly folded form. Several of the misfolded peaks were isolated and found by mass spectrometry to contain three disulfide bonds; however, the retention times were significantly different from the correctly folded form, indicating a different conformation. Sharp, late-eluting peaks were observed for all but two of the acyclic permutants and, based on analysis of αH and βH chemical shifts, represent molecules in which the overall three-dimensional structure and disulfide connectivity of the native circular peptide are retained. Thus, we have shown that it is possible to form the native structure in a range of linear analogues with permuted termini.

The proportion of the late-eluting native peaks to misfolded peaks varied significantly for the different permutants as did the retention times of the native-folded permutants. Amino acid composition had a significant effect on retention time, particularly when the tryptophan residue was removed as seen in Fig. 3 for des-(19–20)-kalata B1. However, retention time also provided a good guide as to how similar a permutant was to the native conformation. For example, Fig. 3 shows that kalata B1(24–23) elutes earlier than the native peptide despite containing the entire amino acid sequence, and thus, the difference in retention time must be accounted for by a conformational change. Structural studies showed that this is associated with disorder in the newly opened loop 6 in this permutant.

The major secondary structure element of kalata B1 is a

distorted triple-stranded β-sheet, which is defined primarily by NOEs between α protons across the strands of the sheet, and hydrogen bonds, which are inferred from slow exchange data. Large $^{3}J_{\alpha HNH}$ coupling constants, which are also indicative of extended structures, are also present in the sheet region. Analysis of NOESY spectra, $^{2}H_{2}O$ exchange data, and $^{3}J_{\alpha HNH}$ coupling constants for the acyclic permutants allowed the extent to which this β-sheet structure is retained to be determined (Fig. 6).

When loops 2, 5, and 6 are cut, a significant amount of the β-sheet structure is retained. Interestingly, the β-hairpin of kalata B1 remains intact when either loop 2 or loop 6 is opened and is partially formed when loop 5 is opened, despite the turn residues being deleted in the latter case. Studies on β-hairpin formation have generally suggested that the turn is formed first, followed by the remaining native hydrogen bonds. However, a recent study suggested that the sheet may propagate outwards following formation of a hydrophobic cluster (34). The results from the present study appear to support the latter conclusion, as des-(19–20)-kalata B1 has the turn residues of the β-hairpin removed but still partially forms the β-hairpin.

As with loops 2, 5, and 6, cutting loop 3 also does not inhibit formation of a folded conformation according to the HPLC data and the αH chemical shifts for des-(12–13)-kalata B1, which suggest it has substantially retained native structure. However this acyclic permutant appears not to be stabilized by hydrogen bonds, as is evident from a lack of slowly exchanging amide protons. Although loop 3 is not directly involved in the distorted triple-stranded β-sheet, it appears to have a significant role in stabilizing the structure through hydrogen bonds.

Analysis of βH shift separations for the acyclic permutants provided valuable structural information, particularly for the cysteine residues, which make up more than half the AMX systems in these molecules. These data confirmed the conclusions from the αH shift analysis that the acyclic permutants with loops 2, 3, 5, and 6 removed largely retained native structure but provided additional details on differences associated with cutting loops 2 or 5 relative to loops 3 or 6, monitored mainly by perturbations to Cys-15 shift separations. It appears that the opening of loops 3 or 6 produces more disorder in the adjacent disulfide bond (Cys-1–Cys-15, labeled as *CysI-CysIV* in Fig. 2) than does the opening of loops 2 or 5, with loop 3 being most critical. Loops 2 (VGGT) and 5 (SWPV) are characterized by two β turns, which are held rigidly together, one below the other, by the adjacent cystine knot core of the molecule. This appears to be the most well defined part of the framework, but its stability appears to be driven by the knot rather than the turns themselves. Removal of these turns causes minimal disruption to the structures.

In most cases there was decreased chemical shift separation of the β protons in the permutants relative to the native peptide, implying more disorder in the permutants; however; Cys-10 and Cys-22, which together form the penetrating disulfide bond of the cystine knot, consistently showed a greater chemical shift separation in the permutants relative to the native peptide. This may reflect strain associated with this bond in the native circular peptide that is relieved in the permutants.

In contrast to the case for loops 2, 3, 5, and 6, when either loop 1 or 4 was opened, the characteristic native folding pattern was not observed on RP-HPLC. This result suggests that the native-like structure was not formed in these two permutants, and it appears likely that the correct disulfide connectivities were not formed. Loops 1 and 4, thus, have a significant role in protein folding. The fundamental difference in folding between acyclic permutants that involve a cut in loops 2, 3, 5, or 6 and those that involve a cut in loops 1 or 4 appears to be related to the integrity of the cystine knot core of these molecules. From Figs. 1 and 2 it is clear that cutting of either loops 1 or 4 results in opening of the embedded ring in the structures formed by disulfide bonds Cys-1–Cys-15 (*I-IV* in Fig. 2) and Cys-5–Cys-17 (*II-V* in Fig. 2) and their connecting backbone segments. The topology diagrams in Fig. 7 show this more clearly. The two outer, or ring-forming, disulfide bonds are represented by *black lines*, with a *shaded line* for the penetrating disulfide bond. When the connection between the outer disulfide bonds is interrupted by the termini of the molecule, as occurs in des-(3)-kalata B1 (**1**) and des-(16)-kalata B1 (**4**), these molecules do not fold. In contrast, when the outer disulfide bonds can be connected to form a ring, the permutants fold into the native conformation, *i.e.* the embedded ring must be intact to allow folding into the native conformation. Furthermore, formation of the complete set of β-sheet interactions (*i.e.* αα NOEs and hydrogen bonds) does not appear to be critical in folding of kalata B1 into a native-like conformation.

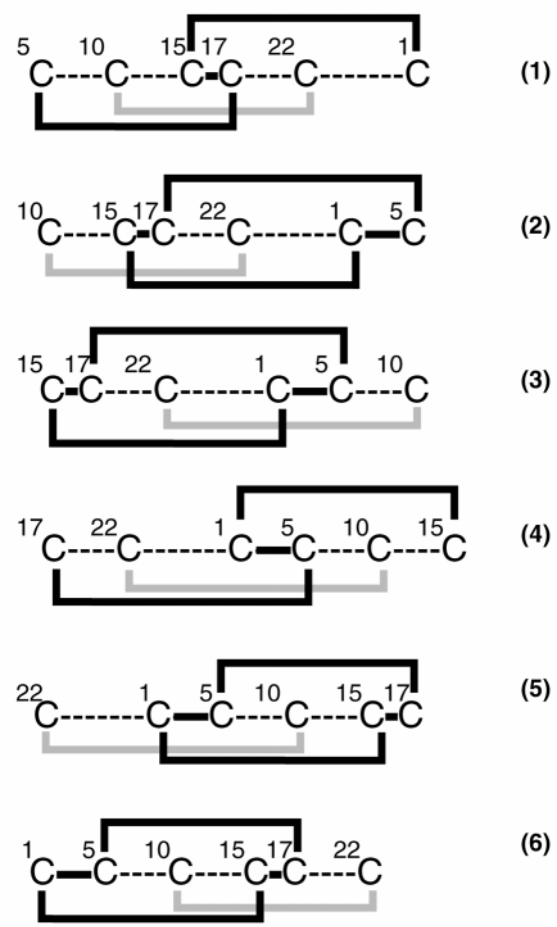

FIG. 7. **A representation of the cystine knot motif in the permutants of kalata B1.** The cysteine residues are *numbered*, and the spacings between each of the cysteine residues are indicated with *dashes*. The disulfide bonds are represented as *lines*, and the core of the cystine knot is highlighted in *thick lines*. The *shaded line* represents the disulfide bond which "threads" through the other two disulfide bonds.

The importance of loops 1 and 4, which make up the connecting segments of the embedded ring, is reflected in their high level of conservation throughout the cyclotide family of macrocyclic peptides (3). Loop 1 (CGE(T/S)C) is conserved throughout the cyclotides. Similarly, loop 4 (C(T/S)C) is also conserved not only in terms of size but also content. The remaining loops in the peptides generally have little homology across the cyclotide family; however, there are some highly conserved sequences

within subsets of these peptides (3, 12). The relative lack of sequence conservation in the remaining loops may reflect a decreased structural importance of these regions, but variability may have evolved associated with various biological activities of different members of the cyclotide family.

The cyclotide peptides exhibit a diverse range of biological activities that originally appeared to be unrelated, ranging from uterotonic to anti-human immunodeficiency virus. However, the hemolytic and anti-microbial activity displayed by several of the peptides (11–13) may give an insight into a common mechanism of action. Membrane disruption is a feature of many hemolytic or antimicrobial compounds and may well explain the other activities of the cyclotides. It was of particular interest in the current study to determine whether a circular backbone *per se* was essential for activity of this family of fascinating proteins.

The acyclic permutants of kalata B1 that folded into the native-like conformation provided an opportunity to assess the effect of opening the circular backbone in topologically different regions on hemolytic activity. Despite having retained the overall three-dimensional structure of the native peptide, as shown by NMR analysis, none of the acyclic permutants was active. Consequently, loss of activity cannot be localized to perturbation of a particular region of the molecule and circularization does indeed appear to be critical. Amide exchange measurements were undertaken to see if flexibility or stability is affected by circularization.

In general, exchange rates of amide protons can provide valuable information on protein stability, folding, and dynamics (35). In the current study we observed an increase in the amide exchange rates in most of the acyclic permutants, suggesting that they are generally more flexible or less stable than the native peptide. Thus, the lack of activity of the permutants in the hemolytic assay may well be a result of increased flexibility. However, other factors must also contribute in individual cases, because the kalata B1(8–7) permutant has similar amide exchange rates to the native peptide but was inactive in the hemolytic assay. In general, though, circularization does appear to increase the stability of the cyclotides.

A recent study on the anti-microbial activity of several macrocyclic peptides from the cyclotide family suggested that their positive charges may be important and that the initial interactions with the microbial surface may be electrostatic (13). This is consistent with hemolytic activity data, as the circulins, which have a higher net positive charge than kalata B1, are more active than kalata B1. Anti-microbial studies also revealed a marked decrease in activity of kalata B1 when its single Arg residue was modified (13). However, the Arg residue of kalata B1 is retained in four of the acyclic permutants that appear to fold into the native-like conformation but are inactive in the hemolytic assay. This suggests that the presence of the Arg residue alone in a native-folded framework does not confer activity.

In summary, we have introduced the concept of acyclic permutation of a circular protein. Using a prototypic member of the cyclotide family, we have shown that cutting the backbone in such as way as to open an embedded ring within the structure disrupts the ability of the molecule to fold. On the other hand cutting the backbone in four of six topologically distinct ways that do not disrupt the cystine knot core does not inhibit folding into native conformations. The study shows that integrity of the core cystine knot is essential to folding and paves the way for further exploitation of the cyclic cystine knot as a template in a diverse range of molecular design applications.

Acknowledgment—We thank Dianne Alewood for some preliminary syntheses.

REFERENCES

1. Boissinot, M., Karnas, S., Lepock, J. R., Cabelli, D. E., Tainer, J. A., Getzoff, E. D., and Hallewell, R. A. (1997) *EMBO J.* **16,** 2171–2178
2. Viguera, A. R., Serrano, L., and Wilmanns, M. (1996) *Nat. Struct. Biol.* **3,** 874–880
3. Craik, D. J., Daly, N. L., Bond, T., and Waine, C. (1999) *J. Mol. Biol.* **294,** 1327–1336
4. Gran, L. (1970) *Medd. Nor. Farm. Selsk.* **12,** 173–180
5. Gran, L. (1973) *Lloydia* (*Cinci.*) **36,** 174–178
6. Gran, L. (1973) *Lloydia* (*Cinci.*) **36,** 207–208
7. Gran, L. (1973) *Acta Pharmacol. Toxicol.* **33,** 400–408
8. Gustafson, K. R., Sowder II, R. C., Henderson, L. E., Parsons, I. C., Kashman, Y., Cardellina, J. H., II, McMahon, J. B., Buckheit, R. W., Jr., Pannell, L. K., and Boyd, M. R. (1994) *J. Am. Chem. Soc.* **116,** 9337–9338
9. Witherup, K. M., Bogusky, M. J., Anderson, P. S., Ramjit, H., Ransom, R. W., Wood, T., and Sardana, M. (1994) *J. Nat. Prod.* (*Lloydia*) **57,** 1619–1625
10. Saether, O., Craik, D. J., Campbell, I. D., Sletten, K., Juul, J., and Norman, D. G. (1995) *Biochemistry* **34,** 4147–4158
11. Schöpke, T., Hasan Agha, M. I., Kraft, R., Otto, A., and Hiller, K. (1993) *Sci. Pharm.* **61,** 145–153
12. Daly, N. L., Love, S., Alewood, P. F., and Craik, D. J. (1999) *Biochemistry* **38,** 10606–10614
13. Tam, J. P., Lu, Y. A., Yang, J. L., and Chiu, K. W. (1999) *Proc. Natl. Acad. Sci. U. S. A.* **96,** 8913–8918
14. Claeson, P., Göransson, U., Johansson, S., Luijendijk, T., and Bohlin, L. (1998) *J. Nat. Prod.* (*Lloydia*) **61,** 77–81
15. Göransson, U., Luijendijk, T., Johansson, S., Bohlin, L., and Claeson, P. (1999) *J. Nat. Prod.* (*Lloydia*) **62,** 283–286
16. Daly, N. L., Koltay, A., Gustafson, K., R., Boyd, M. R., Casas-Finet, J. R., and Craik, D. J. (1999) *J. Mol. Biol.* **285,** 333–345
17. Derua, R., Gustafson, K. R., and Pannell, L. K. (1996) *Biochem. Biophys. Res. Commun.* **228,** 632–638
18. Pallaghy, P. K., Nielsen, K. J., Craik, D. J., and Norton, R. S. (1994) *Protein Sci.* **3,** 1833–1839
19. McDonald, N. Q., and Hendrickson, W. A. (1993) *Cell* **73,** 421–424
20. Daquinag, A. C., Sato, T., Koda, H., Takao, T., Fukuda, M., Shimonishi, Y., and Tsukamoto, T. (1999) *Biochemistry* **38,** 2179–2188
21. Tamaoki, H., Miura, R., Kusunoki, M., Kyogoku, Y., Kobayashi, Y., and Moroder, L. (1998) *Protein Eng.* **11,** 649–659
22. Schnölzer, M., Alewood, P., Jones, A., Alewood, D., and Kent, S. B. H. (1992) *Int. J. Pept. Protein Res.* **40,** 180–193
23. Marion, D., and Wüthrich, K. (1983) *Biochem. Biophys. Res. Commun.* **113,** 967–974
24. Rance, M., Sørensen, O. W., Bodenhausen, G., Wagner, G., Ernst, R. R., and Wüthrich, K. (1983) *Biochem. Biophys. Res. Commun.* **117,** 479–485
25. Braunschweiler, L., and Ernst, R. R. (1983) *J. Magn. Reson.* **53,** 521–528
26. Bax, A., and Davis, D. G. (1985) *J. Magn. Reson.* **65,** 355–360
27. Jeener, J., Meier, B. H., Bachmann, P., and Ernst, R. R. (1979) *J. Chem. Phys.* **71,** 4546–4553
28. Piotto, M., Saudek, V., and Sklenar, V. (1992) *J. Biomol. NMR* **2,** 661–665
29. Chakshusmathi, G., Ratnaparkhi, G. S., Madhu, P. K., and Varadarajan, R. (1999) *Proc. Natl. Acad. Sci. U. S. A.* **96,** 7899–7904
30. Terras, F. R. G., Schoofs, H. M. E., De Bolle, M. F. C., Van Leuven, F., Rees, S. B., Vanderleyden, J., Cammue, B. P. A., and Broekaert, W. F. (1992) *J. Biol. Chem.* **267,** 15301–15309
31. Wüthrich, K. (1986) *NMR of Proteins and Nucleic Acids*, John Wiley & Sons, Inc., New York
32. Kondejewski, L. H., Jelokhani-Niaraki, M., Farmer, S. W., Lix, B., Kay, C. M., Sykes, B. D., Hancock, R. E., and Hodges, R. S. (1999) *J. Biol. Chem.* **274,** 13181–13192
33. Oren, Z., and Shai, Y. (1997) *Biochemistry* **36,** 1826–1835
34. Dinner, A. R., Lazaridis, T., and Karplus, M. (1999) *Proc. Natl. Acad. Sci. U. S. A.* **96,** 9068–9073
35. Englander, S. W., Sosnick, T. R., Englander, J. J., and Mayne, L. (1996) *Curr. Opin. Struct. Biol.* **6,** 18–23

Acyclic Permutants of Naturally Occurring Cyclic Proteins: CHARACTERIZATION OF CYSTINE KNOT AND β-SHEET FORMATION IN THE MACROCYCLIC POLYPEPTIDE KALATA B1

Norelle L. Daly and David J. Craik

J. Biol. Chem. 2000, 275:19068-19075.
doi: 10.1074/jbc.M000450200 originally published online March 27, 2000